

# Patient dose calculation based on ScandiDos Delta<sup>4PT</sup> measurements

Anders Gustafsson, Cureos AB

#### **ABSTRACT**

This paper describes a novel technique for accurate and reliable 3D photon dose calculation in a patient volume based on detector dose measurements in the ScandiDos Delta<sup>4PT</sup> QA phantom.

The technique consists of two steps: (a) for the given beam quality and accounting for the phantom composition, estimate the 2D energy fluence distribution that best represents the measured detector doses in the Delta<sup>4PT</sup> phantom, and (b) apply the obtained energy fluence and the given beam quality in a 3D dose calculation for the patient volume.

The estimated energy fluence distribution represents the radiant energy resulting from modulation and collimation in the treatment head, independent of dose calculation geometry. Presence or absence of flattening filter is automatically accounted for.

The energy fluence estimation is formulated as a linear optimization problem, where the objective is to minimize the integral fluence given that the calculated phantom dose in every accountable detector position is greater than or equal to the measured dose. This formulation is guaranteed to have a feasible solution and the calculated-to-measured dose deviation is implicitly minimized through the integral fluence objective.

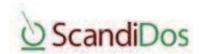
The technique has been applied to both MLC collimated IMRT fields with non-uniform energy fluence and VMAT fields where patient dose is calculated for the individual control points and subsequently added to yield a total 3D dose. The technique is consistently able to reproduce reference absolute dose results within 3% and 3 or 6 mm, depending on the local spatial resolution of the detector grid.

## **INTRODUCTION**

By monitoring beam or control point dose in a large number of small detectors distributed within the ScandiDos Delta<sup>4PT</sup> QA phantom and comparing measured dose with TPS calculated dose *in the phantom*, accurate confirmation of spatial deviations between planned and delivered dose can be obtained.

The clinical interpretation of deviations is however limited by the fact that doses are being compared in the phantom. To facilitate evaluation of the clinical impact of observed dose deviations, the treatment





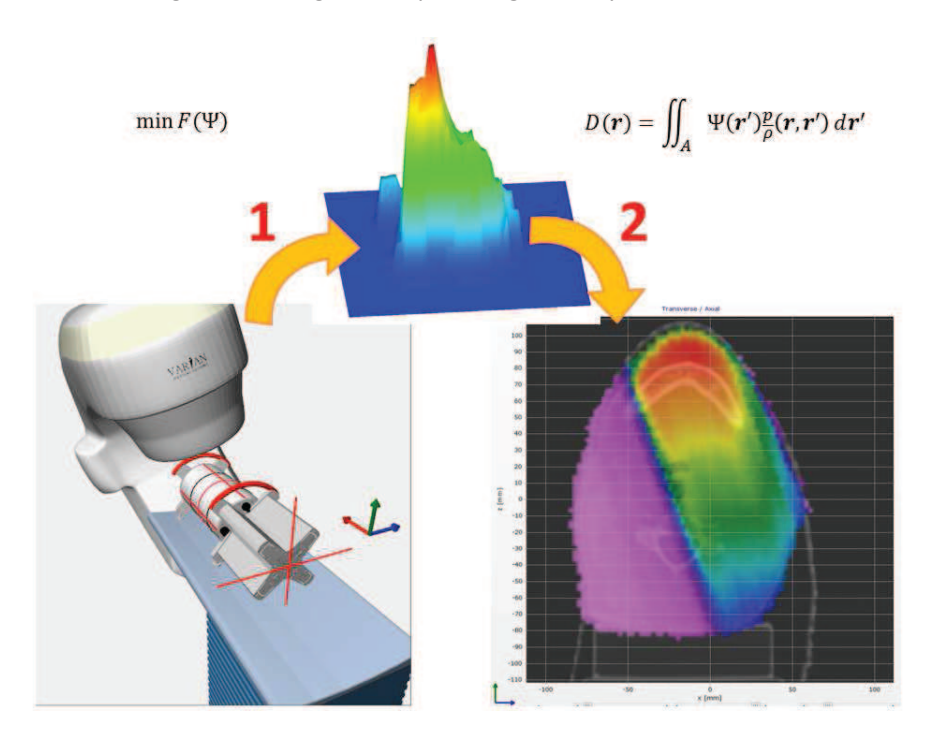
planning system calculated dose *in the patient* should ideally be compared with the patient dose distribution *corresponding to* the measured doses in the ScandiDos Delta<sup>4PT</sup> QA phantom.

#### **METHODS AND MATERIALS**

For each set of measured Delta<sup>4PT</sup> detector doses, for example detector doses recorded for one control point in a VMAT/RapidArc beam or for a composite IMRT beam, the algorithm converts the measured detector doses into the corresponding dose in the associated patient geometry.

For each set of detector doses, the following basic procedure is applied:

- 1. Determine the energy fluence incident on the Delta<sup>4PT</sup> phantom through iterative optimization to yield the best possible correspondence over all detector positions between the measured dose and calculated dose, using the pencil-beam dose algorithm and accounting for phantom geometry and material as well as beam characteristics.
- 2. For the patient geometry of interest, apply the energy fluence obtained in the previous step and calculate dose using the heterogeneous patient geometry and beam characteristics.



# **Energy fluence estimation**

To accurately adopt the point dose measurements in the Delta<sup>4PT</sup> phantom onto a patient geometry, the dose calculation algorithm estimates the energy fluence that produces the measured point doses through optimization. The obtained energy fluence is then used as an input parameter in the dose calculation for a patient geometry.





The energy fluence estimation can be applied both to beams where the energy fluence is relatively homogeneous inside the collimated area and to beams where the energy fluence is highly heterogeneous, for example composite intensity-modulated radiotherapy (IMRT) beams. The energy fluence estimation is furthermore applicable to flattening-filter free beams, and in principle also to physically modulated beams, such as wedge beams. However, the present dose calculation is not able to account for the beam quality changes imposed by physical modulators.

The energy fluence estimation is formulated as the following Linear Programming problem:

$$\begin{aligned} & & & & \sum_{i} \Psi_{i} \\ & & & \\ & & & \\ & & & \\ & & & \\ &$$

where  $\Psi_i$  is the energy fluence, subject to optimization, for a discrete pixel i in the energy fluence distribution,  $D_j$  is the *measured* point dose at position j in the Delta<sup>4PT</sup> phantom and  $d_{ij}$  is the *calculated* absorbed dose per unit energy fluence emanating from energy fluence in pixel i and deposited at position j in the Delta<sup>4PT</sup> phantom. The sums in the "subject to" expressions thus represent the total calculated dose at position j in the Delta<sup>4PT</sup> phantom.

In plain words, the optimization problem can thus be expressed as: find the minimum area integral of the energy fluence given that the calculated dose is larger than or equal to the measured dose in all measurement points in the Delta<sup>4PT</sup> phantom.

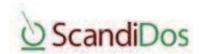
The primary rationale behind this formulation is to limit the dose deposition emanating from distant rays, i.e. only if the calculated dose at a point cannot be sufficiently tailored by nearby rays should farther away rays be allowed to contribute to the calculated dose. Using this principle, the resulting energy fluence will inevitably be concentrated to the volume where the measured dose is significant. There is no explicit upper limit for the calculated dose, but as a side-effect of minimizing the energy fluence area integral the calculated dose excess will still be implicitly limited.

The alternative formulation, to minimize the sum of squared or absolute differences between calculated and measured point doses given that energy fluence is always non-negative, has consciously been avoided here; this alternative approach imposes no restriction to limit the energy fluence from distant rays. It is possible to apply additional restrictions, like for example explicitly requiring energy fluence to be zero in specific regions; these additional restrictions would however be arbitrarily defined, unnecessarily limiting the degrees of freedom for the optimization.

To avoid over-specification of the optimization problem, only a subset of detector dose positions are considered; for each pixel i, the detector position inside the volumetric beam ray for the pixel that is farthest away from the beam source is included in the set of constraints. The rationale for selecting the farthest position is that this position is likely to be least sensitive to inaccuracies in the depth determination.

For energy fluence optimization to deliver sufficient fluence matrices, ideally the volumetric ray of each pixel in the energy fluence matrix should contain *one* or more dose measurement points. If not, and if





not otherwise limited within the scope of the optimization, the magnitude of the fluence pixel without directly corresponding dose measurement points might become unrealistically high as the pixel is attempting to "feed" neighboring dose points with stray dose. To overcome this potential issue while still allowing arbitrary resolution in the energy fluence matrix applied in optimization, the following additional constraints are applied during optimization:

$$\Psi_{\mathbf{k}} = \frac{1}{N_{\mathbf{k}'}} \sum\nolimits_{\mathbf{k}'} \Psi_{\mathbf{k}'}$$

where k represents each energy fluence pixel for which its ray projection does not contain at least *one* dose measurement point (or where the dose measurement point is close to the projected pixel area border), and k' represents an  $N_{k'}$  sized subset of energy fluence pixels *with* associated dose measurement points that are located closest to the projected area of pixel k.

This means that when fluence matrix resolution is fine enough so that not all fluence pixels are directly encompassing a dose measurement point of its own, there will be "clusters" of fluence pixels where the pixels that are encompassing one or more dose measurement points will be actively updated in the optimization, and the neighboring non-encompassing pixels will automatically apply the mean energy fluence magnitude of the closest active pixels.

To solve the linear programming problem for each individual control point or beam, the *lp-solve* Mixed Integer Linear Programming solver software is employed [1].

## Dose calculation algorithm

Dose calculation is based on the photon pencil-beam algorithm described by Ahnesjö *et al* [2]. The algorithm in its current implementation is applicable to:

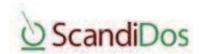
- Linear accelerator generated photon beams, 4-25 MV accelerator potential
- Flattening filter included or excluded in beam production
- Beam collimation using rectangular jaws, multileaf collimators, blocks, apertures

The algorithm is capable of accounting for varying material composition in the patient or phantom geometry, both for tissue represented by Hounsfield numbers as well as specific elements and composite materials relevant in radiotherapy.

More specifically, the algorithm in the ScandiDos Delta<sup>4</sup> software can be outlined as follows:

- 1. Absorbed dose per incident energy fluence is separated into three components, primary, scatter and charged particle contamination (CPC).
- 2. Dose in a single point is calculated by integrating the energy fluence with the primary, scatter and charged particle contamination kernels in a 2D-plane containing the calculation point that is perpendicular to the central axis of the beam.
- 3. Upon integration, primary and CPC kernels are taken at the *radiological* depths of the integration points in the 2D-plane, whereas scatter kernels are taken at the *geometrical* depth.





- 4. Radiological depth is estimated by raytracing through a 3D grid representation of the heterogeneous patient volume to the point of interest based on the raytracing algorithm of Siddon [3].
- 5. In dose calculation of a 3D voxel grid, calculation is separated into a number of 2D-planes perpendicular to the beam axis, and convolution through Fast Fourier Transformation (FFT) is applied to increase calculation speed. In the convolution, primary, scatter and CPC kernels are taken for the energy fluence weighted *average* depths (radiological or geometrical). After completed calculation in the beam-aligned 3D grid, dose in the 3D *display* grid is obtained through nearest-neighbor interpolation in the beam-aligned grid.

#### Primary and scatter dose kernels

The dose calculation algorithm employs the following polyenergetic pencil beam kernel function for energy deposition per unit incident primary photon energy from primary and scatter photons [2]:

$$\frac{p}{\rho}(r,z) = \frac{A_z e^{-a_z r}}{r} + \frac{B_z e^{-b_z r}}{r}$$

where r is the cylindrical radius from the pencil-beam axis and  $A_z$ ,  $a_z$ ,  $B_z$  and  $b_z$  are fitting parameters dependent on the depth z. The first term is defined to represent primary dose and the second term scatter dose.

The fitting parameters  $A_z$ ,  $a_z$ ,  $B_z$  and  $b_z$  can generally be computed with high accuracy using a single beam quality index TPR<sub>20/10</sub> (Tissue Phantom Ratio 20-cm/10-cm) in the index range [0.60, 0.81], approximately corresponding to linear accelerator potentials 3 through 30 MV [4].

In the Delta<sup>4DVH Anatomy</sup> patient dose calculation algorithm, the beam quality index  $TPR_{20/10}$  for a specific linear accelerator and accelerator potential is obtained by fitting measured and calculated depth dose profiles at intermediate to large depths.

#### Charged particle contamination kernels

The dose calculation algorithm employs the following kernel function to represent the energy deposition per unit incident primary photon energy from charged particle contamination [2]:

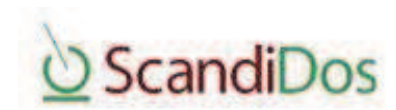
$$\frac{p_{c_{\pm}}}{\rho}(r,z) = \alpha e^{-\beta z} e^{-\gamma r^2}$$

The parameters  $\alpha$ ,  $\beta$  and  $\gamma$  for a specific linear accelerator and accelerator potential are obtained by fitting measured and calculated depth and lateral dose profiles at small depths, accounting for the preestimated beam quality index TPR<sub>20/10</sub>.

#### **Accounting for material heterogeneity**

The primary, scatter and charged particle contamination kernels are defined for a semi-infinite water slab. To account for materials different from water, and following the approach taken in [2], primary and CPC kernels are obtained at the *radiological* depth  $z=z_{\rm rad}$  when applied in the dose calculation. Secondary kernels are obtained at the *geometrical* depth  $z=z_{\rm geom}$  and scaled using a correction factor CF (see Ahnesjö  $et\ al\ [2]$ ).





The radiological depth  $z_{\rm rad}$  is calculated by weighting the traversed distance with the linear attenuation coefficient ratio relative to water for the ray from the radiation source to the geometrical depth of interest.

Attenuation coefficients are energy dependent. The dose calculation implementation contains mass attenuation coefficient  $(\mu/\rho)$  tables for all elements with atomic numbers 1 through 92 as well as tables for a large number of composite materials and alloys that are relevant in radiotherapy. Furthermore, the implementation contains attenuation coefficient tables for a large number of tissue equivalent materials corresponding to different Hounsfield numbers in the regular Hounsfield range [-1000, 3095]. Data is taken from the pre-calculated NIST tables [5], complemented with computation of attenuation coefficients for an additional number of composite materials using the XCOM software, version 3.1 [6].

Using the explicit element and composite material tables along with a runtime Hounsfield number lookup-table, the radiological depths  $z_{\rm rad}$  can be accurately calculated for the entire patient or phantom geometry in the vast majority of cases relevant to radiotherapy.

#### **Raytracing**

To accurately determine geometrical and radiological depths for arbitrary positions in the patient or phantom geometry for an individual beam or control point, the ray-tracing technique of Siddon [3] and subsequently improved by Jacobs *et al* [7] has been applied.

#### 3D dose integration

Internally, the dose calculation is performed in a fine-grained parallel-beam grid that is completely enclosing the patient geometry (as defined by the "radiological path density" grid). The 3D dose calculation is separated into primary, scatter and charged particle contamination calculation of 2D grid planes perpendicular to the beam central axis.

The 3D dose grid generated internally in the dose calculation is aligned with the beam or control point for which dose calculation is requested. This means that the dose grid is beam-centric rather than patient-centric. Before dose contributions from beams (or control points) with different beam geometries can be added, it is thus necessary to transform the beam-centric dose distribution into a patient-centric 3D grid.

The conversion from the parallel-beam geometry to the patient geometry is performed using an affine transformation between the two coordinate systems. The dose in each patient geometry position is interpolated from the nearest neighbors in the parallel-beam geometry.

#### Beam characterization

For patient and phantom dose calculation to yield accurate results, it is required that the beam quality parameters  $\mathsf{TPR}_{20/10}$ ,  $\alpha$ ,  $\beta$  and  $\gamma$  have been sufficiently estimated for the specific beam quality applied in the dose calculation.

The charged-particle contamination parameters  $\alpha$ ,  $\beta$  and  $\gamma$  only affect the absorbed dose at superficial patient/phantom depths, and therefore the beam quality characterization is performed in a two-step process:





- 1. The tissue-phantom ratio parameter  $TPR_{20/10}$  is fitted to yield optimal correspondence between measured and calculated water depth dose profiles below dose maximum for a number of different rectangular field sizes.
- 2. The CPC parameters  $\alpha$ ,  $\beta$  and  $\gamma$  are fitted to yield optimal correspondence between measured and calculated water depth dose profiles near the (phantom) surface for a number of different rectangular field sizes, with TPR<sub>20/10</sub> fixed in the calculation to the value obtained in step 1.

To sufficiently capture the impact of primary versus scatter contribution in the  $\mathsf{TPR}_{20/10}$  estimation for an equivalent energy fluence magnitude in the exposed field, the measured depth dose profiles applied in the characterization should be phantom scatter correction factor  $(S_p)$  normalized, and the (water phantom) depth at which the corresponding total scatter correction factor  $(S_{cp})$  is determined should be large enough not to include charged-particle contamination dose (typically 100 mm, or 50 mm for accelerator potentials below 6 MV).

The  $TPR_{20/10}$  estimation is performed using a one-dimensional optimization algorithm, striving to minimize the sum of squared differences between measured and calculated dose at all measurement depth positions below a specific threshold depth (near dose maximum). The  $\alpha$ ,  $\beta$  and  $\gamma$  estimation is performed using the multi-dimensional bound constrained algorithm BOBYQA [8], striving to minimize the sum of squared differences between measured and calculated dose at all measurement depth positions above a specific threshold depth (below dose maximum) with  $TPR_{20/10}$  fixed to the value obtained in the previous optimization procedure.

#### RESULTS AND DISCUSSION

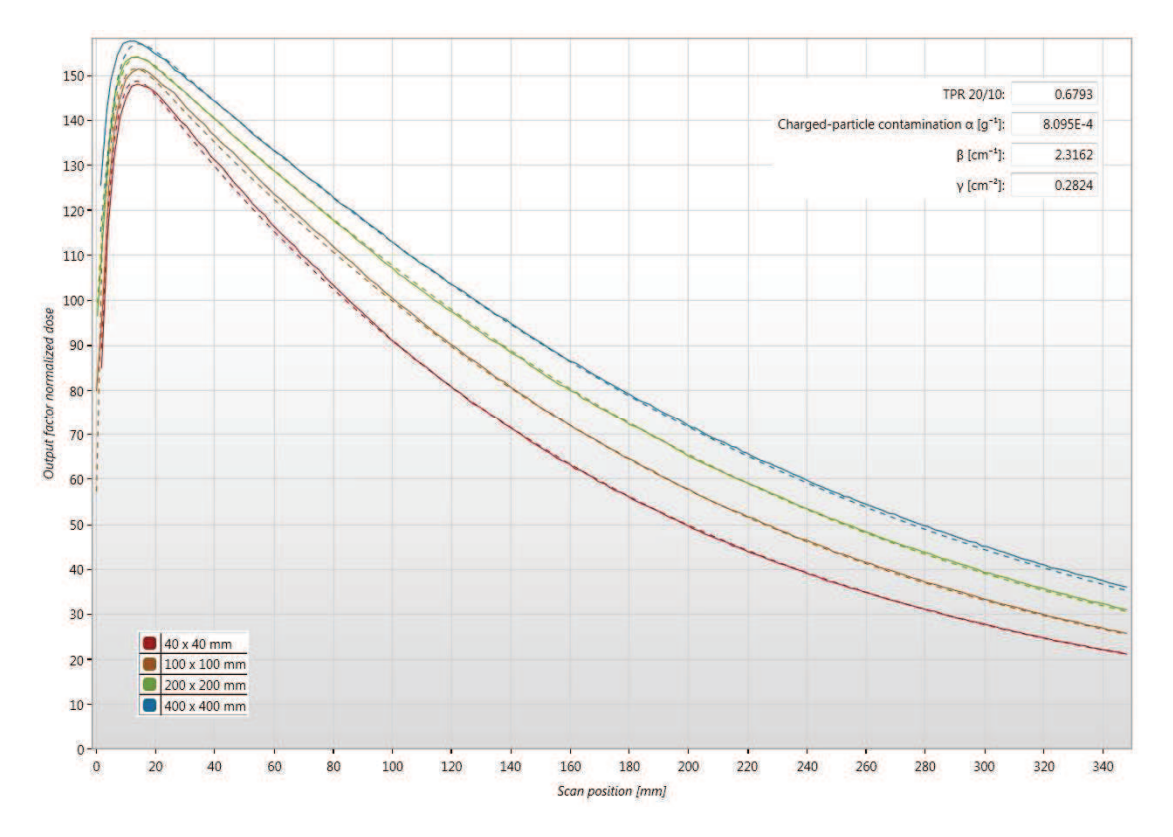
## **Beam characterization**

## Regular beam quality

Given a set of open beam, rectangular field, depth dose profiles and corresponding phantom scatter factors for varying field sizes, a specific beam quality can be sufficiently characterized. The diagram below illustrates the result of a beam characterization for a regular 6 MV beam (solid lines represent measured profiles, dotted lines represent calculated profiles). Agreement between measured and calculated dose is within ±2%/2 mm throughout all field sizes and depths.







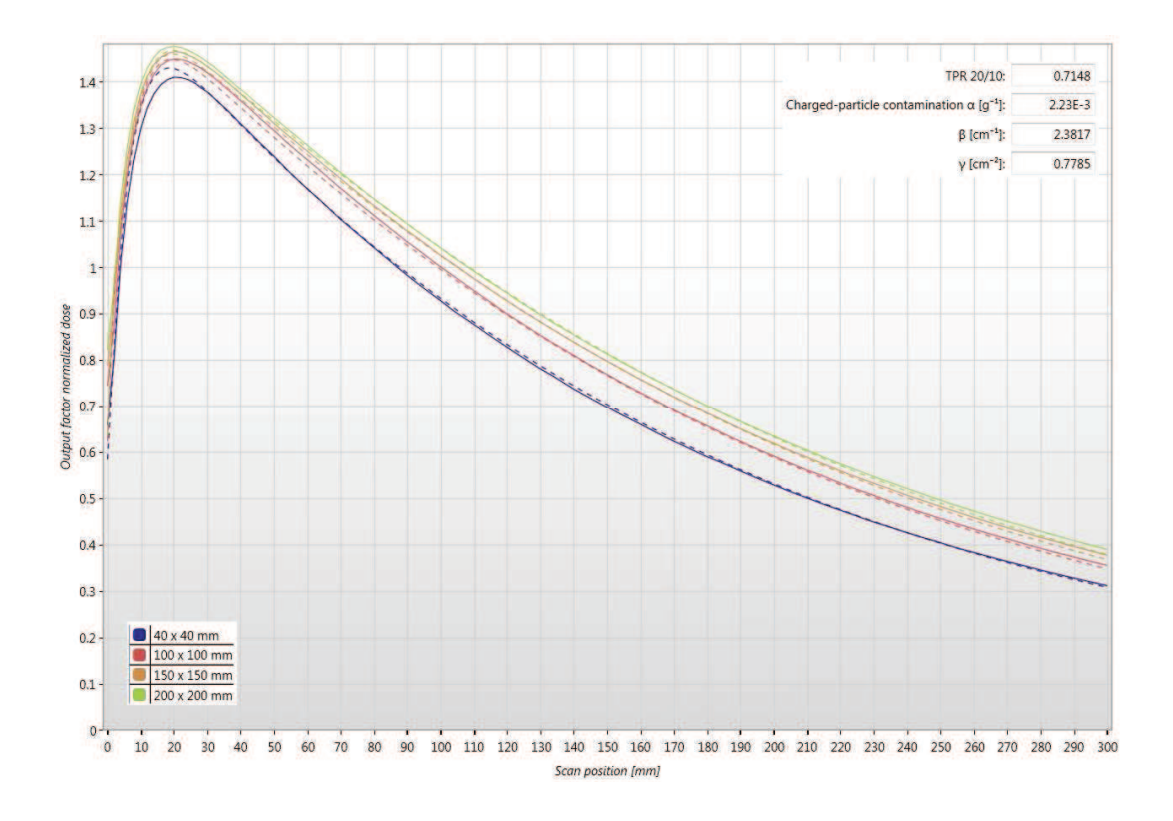
#### Flattening-filter free beam quality

To accurately characterize the quality of a flattening-filter free beam, the lateral energy fluence of the beam is approximated with a radially dependent distribution, decreasing linearly with increasing radius. The slope factor is estimated from a lateral dose profile for a large field at reference depth, using the quotient of dose at a distant off-axis in-field position and the central axis dose.

Accounting for the varying fluence distribution of the flattening-filter free beam, the characterization parameters can be accurately estimated, as is illustrated by this diagram for a 10 MV flattening-filter free beam characterization. Agreement between measured and calculated dose is within  $\pm 3\%/3$ mm throughout all field sizes and depths.







## **Energy fluence optimization**

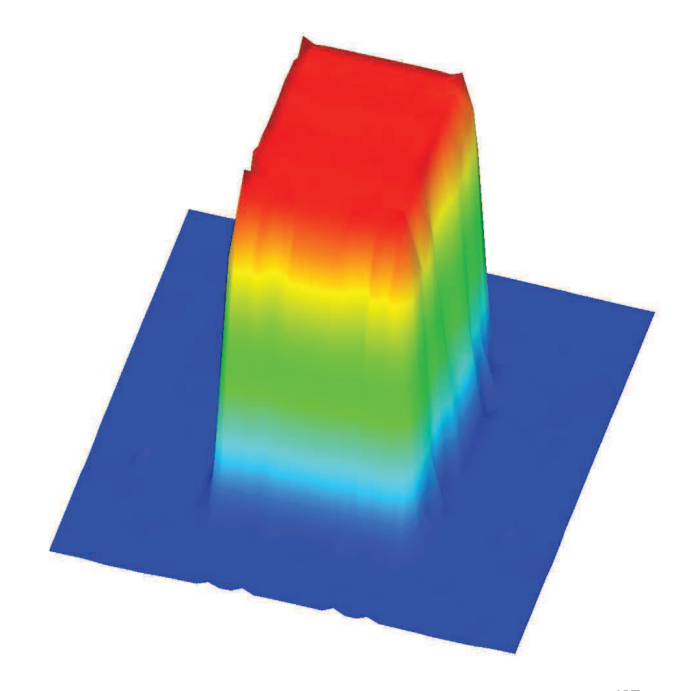
The performance of the energy fluence optimization can be validated by performing optimization for a set of measured doses in the Delta<sup>4PT</sup> phantom detector planes and then evaluating the deviations between calculated and measured dose in the same detector positions.

#### Quadratic field

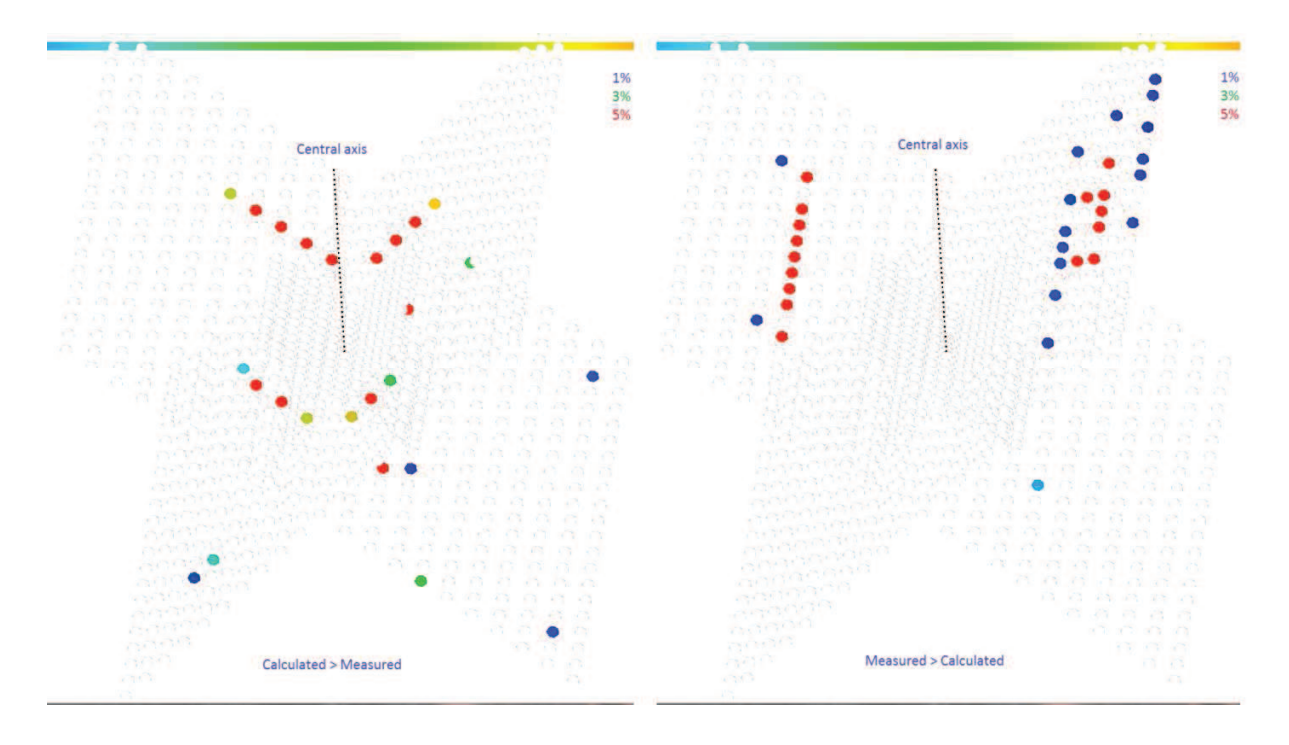
Given a set of measured doses in the Delta<sup>4PT</sup> QA phantom for a 100 mm by 100 mm quadratic 6 MV field, the energy fluence optimization algorithm yields a flat and well defined resulting energy fluence distribution:







The relative deviations between measured and calculated dose in the Delta<sup>4PT</sup> detector positions are in the sub-percent range in the center of the field. Near the field edges the relative deviations range up to 5%, which is primarily due to the limited resolution (6 mm by 6 mm pixels) of the energy fluence grid. It can also be noted that there is a tendency towards calculated underdosage at shallower depths; this is an implicit consequence of primarily using measurement positions farthest from the radiation source in the problem formulation.

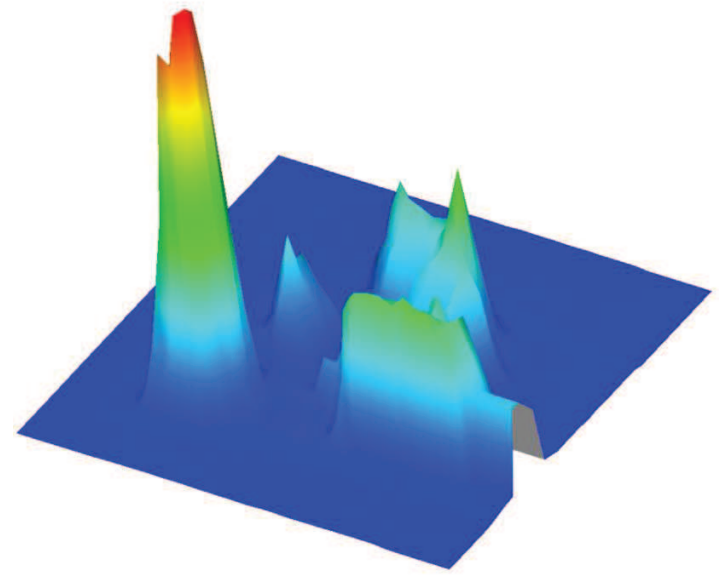




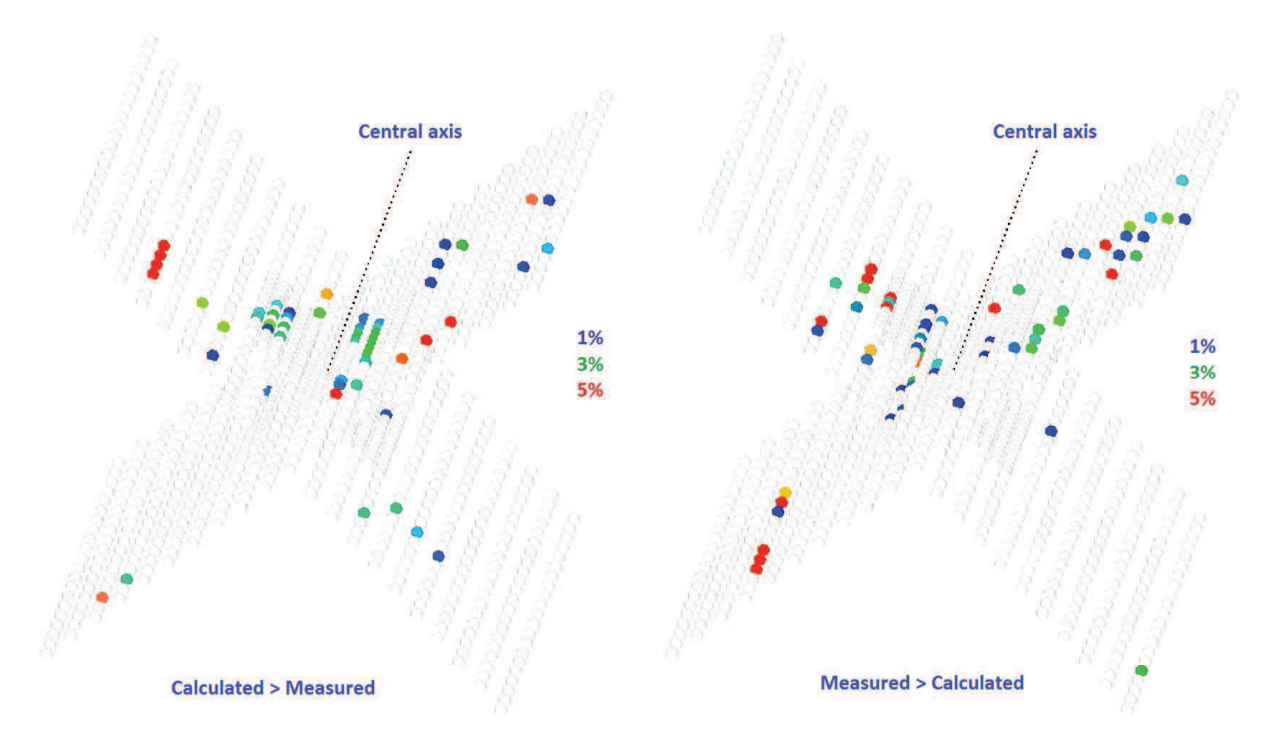


#### **MLC collimated IMRT field**

Given a set of measured doses in the Delta<sup>4PT</sup> phantom for a highly irregular MLC collimated IMRT field, the energy fluence optimization yields a sufficiently inhomogeneous energy fluence distribution:



Due to the highly irregular nature and the limited resolution of the energy fluence matrix, deviations between calculated and measured dose in the Delta<sup>4PT</sup> detector positions are more frequent in the IMRT case than for the quadratic field illustrated above. Deviations are primarily localized to regions of rapid dose changes, indicating distances to agreement less than the pixel size, i.e. <6 mm.







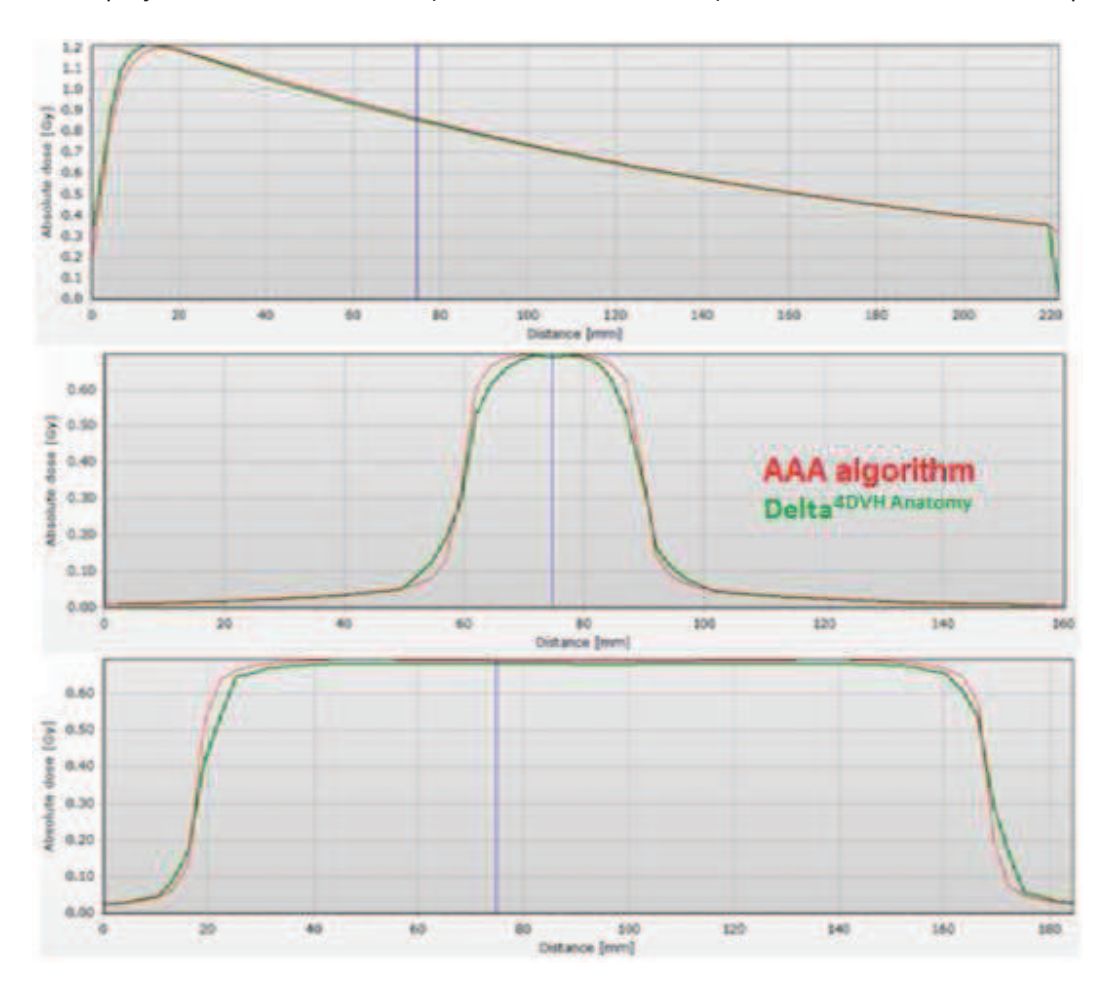
# From measured dose in Delta<sup>4PT</sup> to calculated dose in patient geometry

#### Rectangular elongated field in a water phantom

The feasibility of the composite technique for energy fluence optimization and subsequent patient geometry dose calculation can be justified by irradiating the Delta<sup>4PT</sup> phantom with a rectangular field, using the measured doses in the phantom and the new algorithm to determine the corresponding 3D dose in a water phantom, and comparing this 3D dose with the dose calculated with a regular treatment planning system for the same radiation field and water phantom.

Below is illustrated central axis depth dose profiles and lateral dose profiles at 100 mm depth for the ScandiDos Delta<sup>4DVH Anatomy</sup> patient dose calculation algorithm (green lines) and Varian Eclipse AAA algorithm (red lines) for a 6 MV, 30 mm by 150 mm field in a large water phantom. It can be seen that the absolute dose agreement between Delta<sup>4DVH Anatomy</sup> and Eclipse is well within 2% for this case. In the build-up region there are marked deviations between the two algorithms, which may be attributed to differences in the charged-particle contamination implementations. The penumbrae of the Delta<sup>4DVH</sup>

Anatomy lateral profiles are generally shallower than for the Eclipse lateral profiles, which can be attributed to the projected lateral resolution (5 or 10 mm at isocenter) of the Delta<sup>4PT</sup> measurement positions.

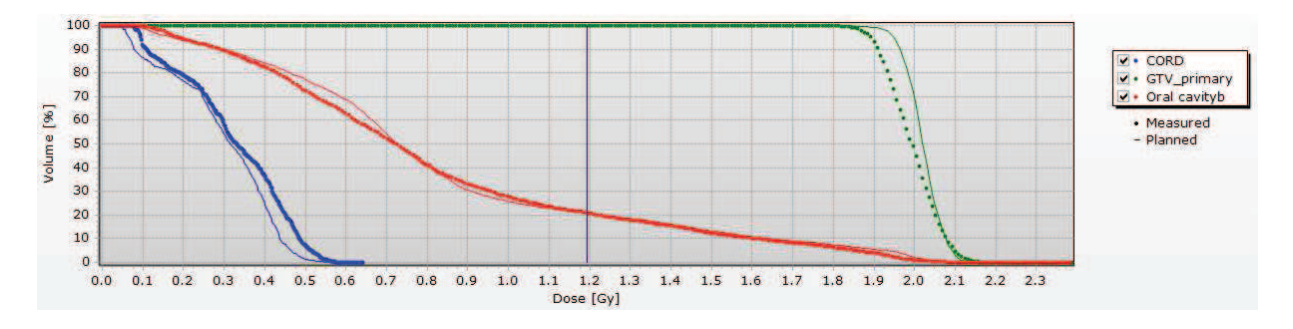






#### Head and neck IMRT treatment

When applied to an oropharynx boost 9 field IMRT treatment, the Delta Patient dose calculation algorithm displays a shallower cumulative dose-volume histogram in the primary GTV than the Varian Eclipse AAA algorithm, but the maximum GTV dose is sufficiently reproduced. The broader GTV dose distribution for the Delta ADVH Anatomy algorithm is primarily a penumbra effect where the algorithm yields penumbrae of the same width as the distance between measurement positions.

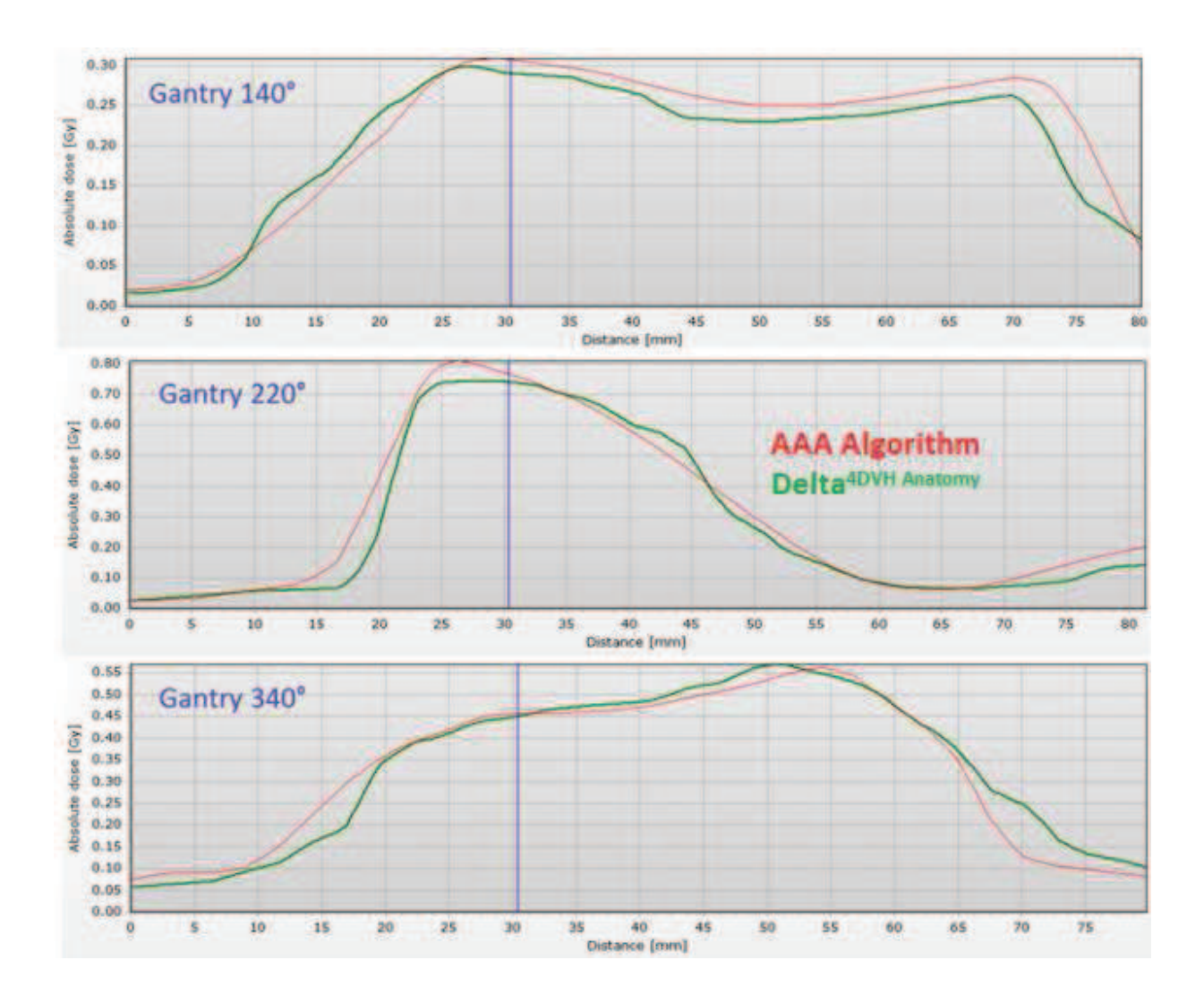


For risk organs close to and distant from the target, the Delta <sup>4DVH Anatomy</sup> patient dose calculation algorithm sufficiently reproduces the dose distributions from the treatment planning system calculation.

Considering a number of lateral dose profiles in the primary GTV for individual beams, it can again be noticed that the Delta<sup>4DVH Anatomy</sup> patient dose calculation algorithm exhibits somewhat shallower penumbrae than the treatment planning system calculation. Overall, the absolute dose levels and lateral variability are however sufficient reproduced:







## **CONCLUSIONS**

A technique for calculating 3D photon dose in the patient volume based on measured detector doses in the ScandiDos Delta<sup>4PT</sup> QA phantom has been implemented. The technique is applicable to complex treatments such as IMRT and VMAT and has been shown to accurately and reliably obtain 3D patient dose distributions that can be immediately compared with 3D dose distributions planned and calculated with a regular treatment planning system.





#### REFERENCES

- [1] M. Berkelaar, J. Dirks, K. Eikland and P. Notebaert, "lp\_solve reference guide," 2013. [Online]. Available: http://lpsolve.sourceforge.net/.
- [2] A. Ahnesjö, M. Saxner and A. Trepp, "A pencil beam model for photon dose calculation," *Medical Physics*, vol. 19, pp. 263-273, 1992.
- [3] R. L. Siddon, "Fast calculation of the exact radiological path for a threedimensional CT array," *Medical Physics*, vol. 12, pp. 252-255, 1985.
- [4] T. Nyholm, J. Olofsson, A. Ahnesjö and M. Karlsson, "Photon pencil kernel parameterisation based on beam quality index," *Radiotherapy and Oncology*, vol. 78, pp. 347-351, 2006.
- [5] J. H. Hubbell and S. M. Seltzer, "NISTIR 5632: Tables of X-Ray Mass Attenuation Coefficients and Mass Energy-Absorption Coefficients from 1 keV to 20 MeV for Elements Z = 1 to 92 and 48 Additional Substances of Dosimetric Interest," National Institute of Standards and Technology, Gaithersburg, MD., 2004. [Online]. Available: http://www.nist.gov/pml/data/xraycoef/.
- [6] M. J. Berger, J. H. Hubbell, S. M. Seltzer, J. Chang, J. S. Coursey, R. Sukumar, D. S. Zucker and K. Olsen, "XCOM: Photon Cross Sections Database (1.5)," National Institute of Standards and Technology, Gaithersburg, MD., 2010. [Online]. Available: http://www.nist.gov/pml/data/xcom/index.cfm.
- [7] F. Jacobs, E. Sundermann, M. Christiaens, B. De Sutter and I. Leamhieu, "A fast algorithm to calculate the exact radiological path through a pixel or voxel space," *Journal of Computing and Information Technology*, vol. 6, no. 1, pp. 89-94, 1998.
- [8] M. J. D. Powell, "DAMTP 2009/NA06: The BOBYQA algorithm for bound constrained optimization without derivatives," Cambridge University Press, Cambridge, 2009.

